2-6-2013

Insertion of Lithium Ions into TiO_2 (rutile) Crystals: An Electron Paramagnetic Resonance Study of the Li-associated Ti^{3+} Small Polaron

A. T. Brant
Air Force Institute of Technology

Nancy C. Giles
Air Force Institute of Technology

Larry E. Halliburton
West Virginia University

Recommended Citation

A. T. Brant, N. C. Giles, L. E. Halliburton; Insertion of lithium ions into TiO2 (rutile) crystals: An electron paramagnetic resonance study of the Li-associated Ti3+ small polaron. Journal of Applied Physics 7 February 2013; 113 (5): 053712. https://doi.org/10.1063/1.4790366

Journal of Applied Physics

RESEARCH ARTICLE | FEBRUARY 06 2013

Insertion of lithium ions into TiO_2 (rutile) crystals: An electron paramagnetic resonance study of the Li-associated Ti^{3+} small polaron

A. T. Brant; N. C. Giles; L. E. Halliburton

Journal of Applied Physics 113, 053712 (2013)
https://doi.org/10.1063/1.4790366

JOURNAL OF APPLIED PHYSICS **113**, 053712 (2013)

Insertion of lithium ions into TiO_2 (rutile) crystals: An electron paramagnetic resonance study of the Li-associated Ti^{3+} small polaron

A. T. Brant,[1,a)] N. C. Giles,[1] and L. E. Halliburton[2]
[1]*Department of Engineering Physics, Air Force Institute of Technology, Wright-Patterson Air Force Base, Ohio 45433, USA*
[2]*Department of Physics, West Virginia University, Morgantown, West Virginia 26505, USA*

(Received 11 December 2012; accepted 21 January 2013; published online 6 February 2013)

Electron paramagnetic resonance (EPR) and electron-nuclear double resonance (ENDOR) are used to identify a Ti^{3+}-Li^+ complex in TiO_2 crystals having the rutile structure. This defect consists of an interstitial Li^+ ion adjacent to a substitutional Ti^{3+} ion (the unpaired electron on the Ti^{3+} ion provides charge compensation for the Li^+ ion). The neutral Ti^{3+}-Li^+ complex is best described as a donor-bound small polaron and is similar in structure to the recently reported neutral fluorine and hydrogen donors in TiO_2 (rutile). Lithium ions are diffused into the crystals at temperatures near 450 °C. Following the diffusion, an EPR spectrum containing groups of four closely spaced lines is observed at 36 K without laser illumination. ENDOR data verify that the four lines within each group are due to a weak hyperfine interaction with one lithium nucleus. Spin-Hamiltonian parameters are obtained from the angular dependence of the EPR spectra. Principal values are 1.9688, 1.9204, and 1.9323 for the g matrix and –2.14, –2.20, and +3.44 MHz for the ^{7}Li hyperfine matrix. © *2013 American Institute of Physics*. [http://dx.doi.org/10.1063/1.4790366]

I. INTRODUCTION

Titanium dioxide (TiO_2) is a unique, multipurpose wide-band-gap semiconductor. In addition to its excellent photocatalytic properties,[1–3] its applications in hydrogen production,[4] and its development as a functioning memristor,[5] this material is also a promising candidate for use as an electrode material in batteries.[6] As a result of its ability to easily accommodate significant concentrations of interstitial lithium ions, TiO_2 has been proposed as a safer and less-expensive alternative to the graphite-based anode materials now being used in lithium-ion batteries. This makes the defect physics involved in the insertion of lithium ions into TiO_2 crystals an important and timely topic. Many fundamental studies, both experimental and computational, have appeared in the literature.[7–18] We focus, in this report, on an experimental investigation of the local charge compensation mechanism that occurs when lithium ions are inserted into TiO_2 (rutile) crystals.

The physics and chemistry of point defects in TiO_2 are complex and challenging subjects and they continue to be an active area of research for both the rutile and anatase phases of the material. A series of Ti^{3+} centers, each slightly different from the others, are a core aspect of the defect-mediated functionality associated with this versatile semiconductor.[19] In particular, these trapped-electron centers are easily formed in single crystals during reducing treatments or at low temperature with laser light, and they all have a substitutional Ti^{3+} ion as a central component. It is not surprising that much of the defect behavior of TiO_2 is related to the properties of these centers. The Ti^{3+} ions, with their unpaired spins, are best studied using electron paramagnetic resonance (EPR) and electron-nuclear double resonance (ENDOR). In previous investigations of rutile-structured TiO_2 crystals, EPR and ENDOR were used to experimentally establish ground state models of the singly ionized and neutral charge states of oxygen vacancies[20,21] and the neutral charge states of fluorine and hydrogen donors,[22,23] all of which are Ti^{3+}-associated defects.

In the present paper, we describe the results of an EPR and ENDOR investigation of neutral Ti^{3+}-Li^+ centers in TiO_2 (rutile) single crystals. After diffusing lithium into a crystal, an $S = 1/2$ EPR spectrum exhibiting a small hyperfine interaction with an $I = 3/2$ nucleus is observed at low temperature. ENDOR clearly identifies ^{7}Li as the participating nucleus, and the g matrix and the ^{7}Li hyperfine matrix are obtained from the angular dependence of the EPR spectrum. These spin-Hamiltonian parameters establish the ground-state model for the Ti^{3+}-Li^+ center. A Li^+ ion occupies an interstitial position adjacent to a substitutional Ti^{3+} ion, thus forming a neutral paramagnetic complex. This model is similar to those previously determined for the neutral fluorine and hydrogen donors in bulk TiO_2 crystals.[22,23] All three of these defects (i.e., a substitutional Ti^{3+} ion adjacent to fluorine, hydrogen, or lithium) are appropriately described as donor-bound small polarons.[24]

II. EXPERIMENTAL DETAILS

The TiO_2 crystals used in this study have the rutile structure and were commercially grown at CrysTec (Berlin, Germany) by the Verneuil technique. As shown in Fig. 1, the tetragonal TiO_2 (rutile) crystal lattice consists of distorted TiO_6 octahedra. These octahedra are alternately elongated in the [110] and [$\bar{1}$10] directions, with the two orientations related by a 90° rotation about the [001] direction. The six oxygen ions in an octahedron divide into two groups; two of these ions are located along the elongation direction and the

a)Author to whom correspondence should be addressed: Electronic mail: Adam.Brant.ctr@afit.edu.

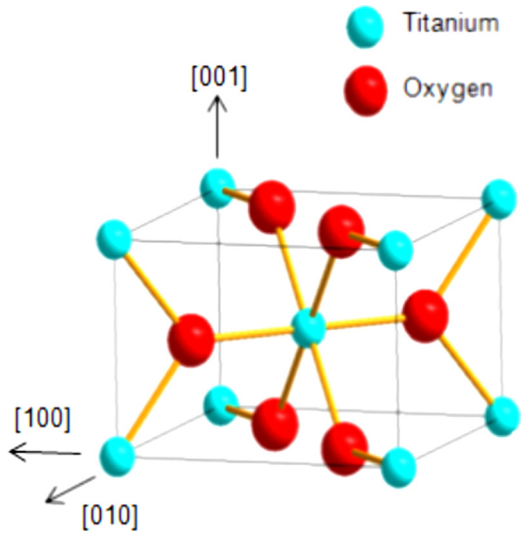

FIG. 1. Tetragonal crystal structure of TiO_2 (rutile). One of the two equivalent TiO_6 octahedra is illustrated.

other four ions are located in the plane perpendicular to the elongation direction.

Samples for the EPR and ENDOR experiments had dimensions of $3 \times 3 \times 2\,mm^3$ and were cut from a larger $10 \times 10 \times 2\,mm^3$ plate provided by CrysTec. The as-received crystal was undoped and clear to the eye. As expected, EPR signals from trace amounts of Fe^{3+} and Cr^{3+} were observed in the as-received crystal. The following procedure was used to diffuse lithium into the TiO_2 crystals. A sample was completely surrounded with LiOH powder in a small ceramic boat. The boat containing the immersed sample was then placed in a furnace that had been preheated to 450 °C. It was held at this elevated temperature for an extended time (4–18 h), while exposed to the atmosphere (i.e., air). After diffusing in lithium, the sample appeared brown to the eye.

The EPR data were taken using a Bruker EMX spectrometer and the ENDOR data were taken using a Bruker E-500 spectrometer. Both spectrometers operated at microwave frequencies near 9.5 GHz. Oxford helium-gas flow systems controlled the temperature of the samples in the 10–40 K range. A proton NMR gaussmeter was used to measure the static magnetic fields. Corrections for the small difference in field strength between the position of the sample and the tip of the gaussmeter probe were obtained by placing a Cr-doped MgO crystal in the microwave cavity at the same position originally occupied by the TiO_2 sample. The isolated Cr^{3+} ions in MgO have an isotropic g value of 1.9800.

III. EPR AND ENDOR RESULTS

Prior to the in-diffusion of lithium ions, the EPR signals initially reported by Yang *et al.*[20,25] could be photoinduced at 25 K in our as-received TiO_2 crystals using 442 nm light from a He-Cd laser. These included the lines assigned to singly ionized and neutral oxygen vacancies and the line assigned to Ti^{3+}-Si^{4+} centers. After diffusing in Li ions, the EPR line assigned to the Ti^{3+}-Si^{4+} center and a new four-line defect were observed at low temperature without illumination, while the signals from the singly ionized and neutral oxygen vacancies still required illumination to be seen at 25 K. This suggests that the Fermi level moved higher in the lithium-treated samples, but not sufficiently high to populate the paramagnetic charge states of the oxygen vacancies in the absence of light.

The EPR spectra shown in Fig. 2 were obtained (without illumination) from a TiO_2 crystal that had been held at 450 °C for 18 h in LiOH powder. These data were taken at 36 K. In Fig. 2(a), the magnetic field is along the [100] direction of the crystal. In Fig. 2(b), the magnetic field is rotated 5° away from the [100] direction while remaining in the basal plane of the crystal. The EPR signals at 348.9 mT in Fig. 2(a) and at 348.2 and 349.6 mT in Fig. 2(b) are from the Ti^{3+}-Si^{4+} center[20,25] and will not be further discussed in this paper. Instead, we focus on the new spectrum consisting of sets of four lines in Figs. 2(a) and 2(b). This EPR spectrum, with linewidths of 0.03 mT at 36 K, becomes broad and difficult to detect when the temperature is above 50 K. The different sets of four lines in Figs. 2(a) and 2(b) are due to magnetically inequivalent, but crystallographically equivalent, orientations of the responsible defect. These magnetically inequivalent orientations occur because of the anisotropy of the g matrix. There are two

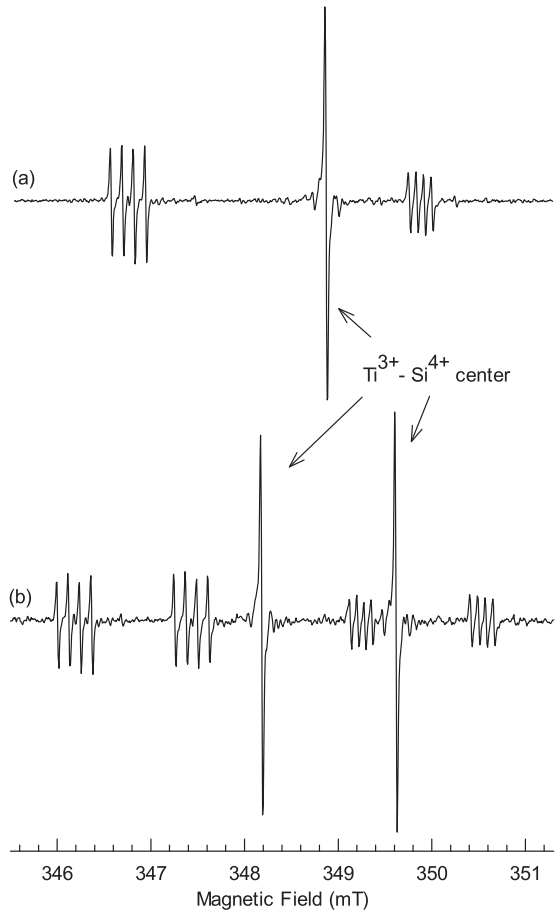

FIG. 2. EPR spectrum of the Ti^{3+}-Li^{+} center in TiO_2 (rutile) with its separate sets of four lines due to a ^7Li hyperfine interaction. As indicated, the single lines are due to the Ti^{3+}-Si^{4+} center. These data were taken at 36 K with a microwave frequency of 9.481 GHz. (a) The magnetic field is along the [100] direction. (b) The magnetic field is 5° away from the [100] direction while remaining in the basal plane.

magnetically inequivalent orientations in Fig. 2(a) and four magnetically inequivalent orientations in Fig. 2(b). All orientations of the defect are magnetically equivalent when the magnetic field is along the [001] direction and only one set of four lines is observed.

Based on the observed negative g shifts (i.e., g values less than 2.0023) and resolved hyperfine patterns, the spectrum with groups of four lines in Fig. 2 is assigned to a Ti^{3+} ion interacting with a ^7Li nucleus ($I = 3/2$, 92.5% abundant). Evidence for the participation of lithium is twofold. First, the spectrum was not present in TiO_2 crystals before diffusing in the lithium. Second, the ENDOR results in Sec. III B unambiguously identify ^7Li as the nucleus responsible for the sets of four lines. We use the notation Ti^{3+}-Li^+ as a label for this EPR-active neutral complex. The Ti^{3+} ion occupies a regular Ti^{4+} site and the associated Li^+ ion occupies an adjacent interstitial site located near the center of the open channel running along the c axis (i.e., the [001] direction) of the crystal. The unpaired spin is localized on the titanium ion (making it a $3d^1$ ion with $S = 1/2$) and the close proximity of the interstitial Li^+ ion gives rise to a weak, but easily observed, hyperfine interaction.

A model of the Ti^{3+}-Li^+ center is shown in Fig. 3 for one of the two equivalent TiO_6 octahedra in the rutile lattice. The Ti^{3+} ion, the Li^+ ion, and the oxygen ion along the [110] elongation direction are all in the same (001) plane, and the Li^+ ion is located along the [100] direction extending out from the Ti^{3+} ion. The other oxygen ions in Fig. 3 are above and below the (001) plane that contains the Ti^{3+} and Li^+ ions. There are four equivalent, and equally possible, locations for the interstitial Li^+ ion adjacent to the Ti^{3+} ion in this TiO_6 octahedron (i.e., the Li^+ ion can be along the [100], [010], [$\bar{1}$00], or [0$\bar{1}$0] directions). The second TiO_6 octahedron in the rutile lattice, rotated by 90° about the [001] direction, also has four possible locations of the interstitial Li^+ ion next to its central Ti^{3+} ion.

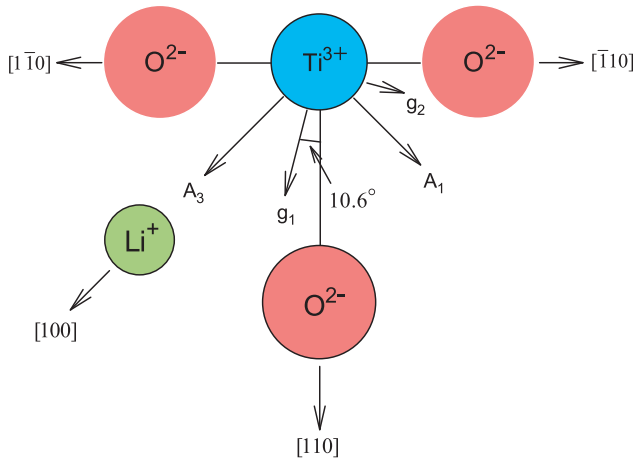

FIG. 3. Model of the Ti^{3+}-Li^+ center in TiO_2 (rutile) showing a substitutional Ti^{3+} ion and an interstitial Li^+ ion. This is a projection on the (001) plane of the TiO_6 octahedron that is elongated along the [110] direction. The lower oxygen ion (with a solid border) is in the same plane as the Li^+ and Ti^{3+} ions, while the left and right oxygen ions (with no solid border) are above and below this plane. The two oxygen ions above the plane overlap the two oxygen ions below the plane.

The g matrix and the ^7Li hyperfine matrix reported in this paper support the model of the Ti^{3+}-Li^+ center presented in Fig. 3. As shown in this figure, two principal axes of the g matrix are in the basal plane, where they deviate slightly (≈10.6°) from the [110] and [$\bar{1}$10] directions, and one principal axis is along the [001] direction. For the ^7Li hyperfine matrix, two principal axes are again in the basal plane along the [100] and [010] directions and one principal axis is along the [001] direction. Although both matrices have a principal axis along the [001] direction, their principal-axis directions do not coincide in the basal plane. The g matrix has a principal axis in the basal plane that is closely aligned with the direction from the Ti^{3+} ion to its neighboring elongated oxygen ion, while the ^7Li hyperfine matrix has a principal axis in the basal plane that is along the line joining the Ti^{3+} and Li^+ ions. As expected, the neighboring oxygen ions dominate the g matrix directions, while the position of the lithium ion strongly influences the ^7Li hyperfine matrix directions.

A. Determination of the g matrix

The parameters describing the g matrix of the Ti^{3+}-Li^+ center are determined from the angular dependence of the EPR spectrum. Experimental data corresponding to the mid-points of each four-line group in the spectrum are plotted as discrete points in Fig. 4. By plotting only the mid-points of these groups we remove information about the ^7Li hyperfine interaction from the figure. Data were not obtained for some directions of magnetic field because of interference from the Ti^{3+}-Si^{4+} center. The angular dependence in Fig. 4 requires one principal axis of the g matrix to be along the [001] direction in the crystal and the other two principal axes to be in the basal plane, but not along the high-symmetry directions of the crystal. This set of principal-axis directions predicts eight crystallographically equivalent orientations of the g matrix (i.e., eight orientations of the Ti^{3+}-Li^+ defect). The eight distinct orientations of the g matrix principal-axis

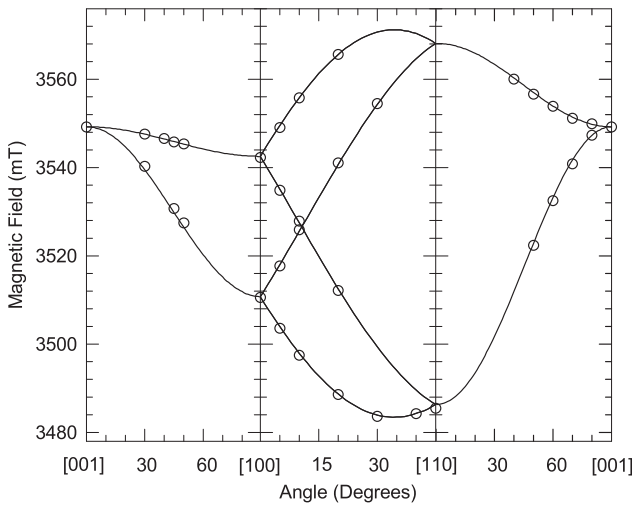

FIG. 4. Angular dependence of the g matrix in the (010), (001), and ($\bar{1}$10) planes. The discrete points are experimental data and the solid lines are generated using the g matrix parameters in Table I and a microwave frequency of 9.599 GHz.

directions arise because of the eight possible positions of the Li^+ ion in the two TiO_6 octahedra. All eight of these crystallographically equivalent orientations of the *g* matrix are magnetically equivalent when the magnetic field is along the [001] direction. The eight crystallographically equivalent orientations separate into two magnetically inequivalent orientations when the magnetic field is along the [100] direction, as shown in Fig. 2(a). There are two magnetically inequivalent orientations for the [110] direction of field and four magnetically inequivalent orientations for an arbitrary direction of field in the basal plane (this latter case is shown in Fig. 2(b)). The magnetically inequivalent orientations of the *g* matrix are reflected in the angular dependence shown in Fig. 4.

The following spin Hamiltonian describes the EPR spectrum of the Ti^{3+}-Li^+ center.

$$\mathbf{H} = \beta \mathbf{S} \cdot \mathbf{g} \cdot \mathbf{B} + \mathbf{I} \cdot \mathbf{A} \cdot \mathbf{S} - g_N \beta_N \mathbf{I} \cdot \mathbf{B} \quad (1)$$

Only the electron Zeeman term is used when determining the *g* matrix. Since one principal axis of the *g* matrix is along the [001] direction, four parameters (three principal values and one angle in the basal plane) are sufficient to describe the *g* matrix. A least-squares fitting routine provided the final numerical values for these parameters. Input data consisted of the 35 experimental magnetic field values plotted in Fig. 4 and their corresponding microwave frequencies. The "best-fit" *g* matrix parameters are listed in Table I. These final values were used to generate the solid lines in Fig. 4.

B. Verification of the ^{7}Li hyperfine assignment

An ENDOR spectrum from the Ti^{3+}-Li^+ center is shown in Fig. 5. These data were taken at 20 K with the magnetic field along the [001] direction. The magnetic field was held constant at 352.42 mT and the microwave frequency was 9.532 GHz. This corresponds to the next-to-lowest-field EPR line in the [001] spectrum. Two ENDOR lines, at 4.78 and 6.93 MHz, are present in Fig. 5. These same two ENDOR lines were observed when the magnetic field was fixed at each of the other three EPR lines in the [001] spectrum (i.e., no additional ENDOR lines were resolved). This verifies that the nuclear electric quadrupole interaction is too weak to be resolved. The hyperfine interaction represented by the two lines in Fig. 5 is small, thus the two lines are centered on the Larmor frequency ν_n of the responsible nucleus and are separated by the hyperfine parameter A.[26] The midpoint of the two lines is 5.85 MHz, which is very close to the known value of 5.83 MHz for the ν_n value of the ^{7}Li nucleus at the fixed magnetic field where the ENDOR spectrum was taken. This good agreement provides conclusive evidence that a ^{7}Li nucleus is responsible for the four-line EPR hyperfine patterns in Fig. 2. The two ENDOR lines in Fig. 5 are separated by 2.15 MHz, which is consistent with the splitting of 0.081 mT that occurs between the EPR lines in the [001] spectrum.

TABLE I. Spin-Hamiltonian parameters for the Ti^{3+}-Li^+ center in TiO_2 (rutile) crystals. The labeling and directions correspond to the schematic model of the defect shown in Fig. 3. Estimated error limits are ±0.0002 for the g values, ±0.10 MHz for the A values, and ±2.0° for the directions.

	Principal Values	Principal-Axis Directions
g matrix		
g_1	1.9688	10.6° from [110] toward [100]
g_2	1.9204	10.6° from [$\bar{1}$10] toward [010]
g_3	1.9323	[001]
^{7}Li hyperfine matrix		
A_1	–2.14 MHz	[010]
A_2	–2.20 MHz	[001]
A_3	+3.44 MHz	[100]

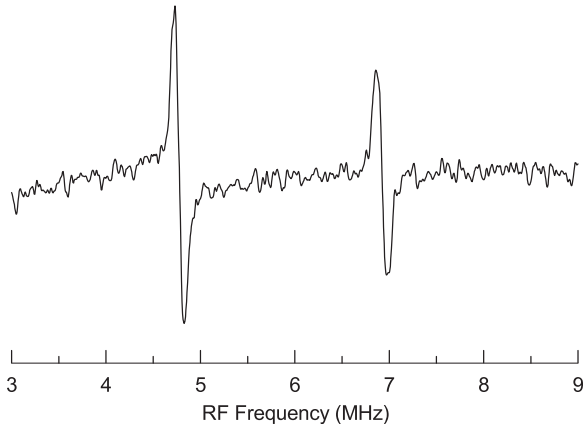

FIG. 5. ENDOR spectrum from the Ti^{3+}-Li^+ center. These data were taken at 20 K with the magnetic field along the [001] direction. The microwave frequency was 9.532 GHz and the magnitude of the magnetic field was 352.42 mT.

C. Determination of the ^{7}Li hyperfine matrix

The angular dependence within the four-line EPR groups (like those illustrated in Fig. 2) was used to determine the ^{7}Li hyperfine matrix. ENDOR spectra were not used to establish this matrix because unfavorable spin-lattice relaxation times prevented ENDOR spectra from being acquired for many directions of magnetic field. Figure 6 is a plot of the average separation within the sets of four EPR lines when the magnetic field was rotated in the (010), (001), and ($\bar{1}$10) planes of the crystal. Both positive and negative values occur along the vertical axis in Fig. 6 because there are several instances where the four lines in a set "cross over" each other (i.e., the separation becomes zero and their ordering reverses as the "effective" sign of the hyperfine interaction changes). The angular dependence of the ^{7}Li hyperfine matrix in Fig. 6 is simpler than the angular dependence of the *g* matrix in Fig. 4. This difference occurs because the two principal-axis directions of the ^{7}Li matrix in the basal plane are along the [100] and [010] directions (see Fig. 3). Thus, there are only two, instead of four, magnetically inequivalent orientations of the ^{7}Li matrix for the rotation from [100] to [110] (the middle panel in Fig. 6). Similarly, there is only one, instead of two, magnetically inequivalent orientations of the ^{7}Li matrix for the rotation from [110] to [001] (the right panel in Fig. 6).

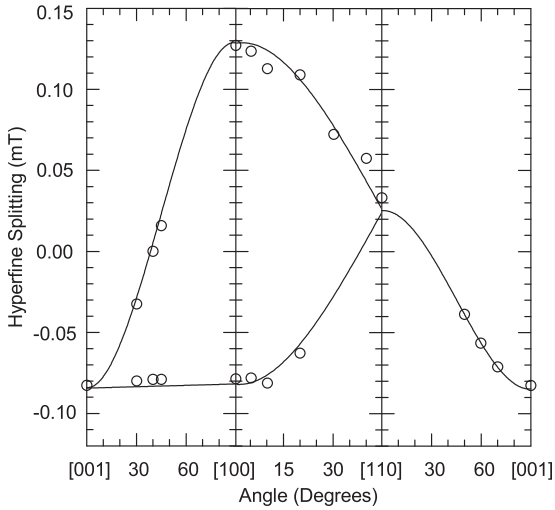

FIG. 6. Angular dependence of the ^{7}Li hyperfine matrix in the (010), (001), and ($\bar{1}$10) planes. The discrete points are experimental data and the solid lines are generated using the hyperfine parameters in Table I.

The hyperfine term in the spin Hamiltonian, see Eq. (1), was used to determine the parameters describing the ^{7}Li hyperfine matrix. Because the principal-axis directions are along high-symmetry directions in the crystal, it is relatively simple to extract the three principal values of the ^{7}Li hyperfine matrix from the data presented in Fig. 6. One of the principal values is obtained from the average splitting in the four line group observed when the magnetic field is along the [001] direction. The other two principal values are obtained from the average splittings for the two separate four-line groups that are observed in Fig. 2(a) when the magnetic field is along the [100] direction. The "best" values for the ^{7}Li hyperfine parameters are listed in Table I and are used to generate the solid curves in Fig. 6. Only the relative signs of the hyperfine parameters can be determined from the EPR data. Since the anisotropic (dipole-dipole) interaction dominates this hyperfine matrix, we choose signs for these parameters that reflect the positive ^{7}Li nuclear magnetic moment. As shown in Fig. 3, the point dipole-dipole nature of the hyperfine matrix requires the direction of the principal axis associated with the +3.44 MHz principal value to be along the [100] direction, i.e., along the line joining the Ti^{3+} ion and the Li^+ ion. This, in turn, requires the direction associated with the g_1 principal value in Fig. 3 to be between the [100] and [110] directions. This direction of g_1 relative to A_3 in Fig. 3 is in agreement with the data in Fig. 2(a) where the lower-field set of four lines has a larger hyperfine splitting than the higher-field set of four lines.

IV. DISCUSSION

Charge neutrality for the crystal as a whole must be maintained when interstitial Li^+ ions are inserted into a TiO_2 crystal. This requires that electrons also enter the crystal during the diffusion process. Once they are in the crystal, an electron and a Li^+ ion do not combine to form a Li^0 ($1s^22s$) atom because a large amount of energy is needed to populate a lithium 2s orbital. Instead, the electron that compensates an interstitial Li^+ ion is localized on one of the nearest Ti^{4+} ions and creates a Ti^{3+} ion. The minimum energy (i.e., the greatest binding energy) occurs when the interstitial Li^+ ion and the substitutional Ti^{3+} ion are immediately adjacent to each other. The resulting Ti^{3+}-Li^+ complex can be described as a donor-bound small polaron.[24] The ground state configuration of this defect is confirmed in the present paper. A similar lithium-related defect was observed with EPR in crystalline SiO_2 (quartz) by Jani *et al.*[27] The defect reported by those authors has an electron localized on a silicon ion and a small, but well-resolved, hyperfine interaction with an adjacent interstitial lithium ion.

The ^{7}Li hyperfine matrix provides the needed information to establish the location of the Li^+ ion in the Ti^{3+}-Li^+ center. As can be seen in Table I and Fig. 3, this hyperfine matrix is nearly axial and has its unique principal axis along a [100] direction. This is the direction pointing from a Ti^{3+} ion toward the middle of the "open [001] channel" in this lattice. The hyperfine matrix is separated into isotropic and anisotropic parts in the following equation:

$$\overleftrightarrow{A} = \begin{pmatrix} a-b+b' & 0 & 0 \\ 0 & a-b-b' & 0 \\ 0 & 0 & a+2b \end{pmatrix}. \qquad (2)$$

The parameter a is the Fermi contact term, b is the primary dipole-dipole interaction, and b' is a small nonaxial anisotropic contribution. Using the results for A_1, A_2, and A_3 in Table I, we obtain $a = -0.30$ MHz, $b = +1.87$ MHz, and $b' = +0.03$ MHz. The small magnitude of the Fermi contact parameter a indicates that the contribution to the hyperfine matrix from a 2s orbital on the Li^+ ion is close to zero.[28,29] Interestingly, the parameter a has the opposite sign of the ^{7}Li nuclear magnetic moment. This negative sign may arise from an exchange polarization of the core electrons on the Li^+ ion.[30] As expected, the classical dipole-dipole interaction is the dominant contributor to the ^{7}Li hyperfine matrix. Treating the +1.87 MHz value of b as the interaction of two point dipoles, one from the unpaired electron centered at the Ti^{3+} ion and the other from the magnetic moment of the ^{7}Li nucleus, gives a separation distance of 2.54 Å. This compares well with the known value of 2.30 Å for the distance in the perfect lattice from a titanium ion to the center of the adjacent [001] channel. Thus, the anisotropic portion of the ^{7}Li hyperfine matrix verifies that the Li^+ ion is located near the middle of this channel and is in the same (001) plane as the Ti^{3+} ion. This places the Li^+ ion in a "cage" consisting of six nearest-neighbor oxygen ions. These six oxygen ions separate into a set of two and a set of four, and are located 1.663 and 2.225 Å, respectively, from the center of the cage. There are also six nearest-neighbor titanium ions around the perimeter (one being the Ti^{3+} ion). It is possible that the Li^+ ion will take a position slightly off-center in this cage.

The principal values of the g matrix reported in Table I for the Ti^{3+}-Li^+ center are similar to those previously found for the fluorine[22] and hydrogen[23] donors in TiO_2 (rutile). This is not surprising since the unpaired spin in all three defects is primarily localized in a d orbital on a Ti^{3+} ion. For comparison, the principal values of these three defects are listed in Table II. Their relative magnitudes do not follow

TABLE II. Comparison of the principal values of the g matrices for a set of donor-bound small polarons (i.e., perturbed Ti^{3+} centers) in TiO_2 (rutile) crystals. These are substitutional Ti^{3+} ions that have an adjacent perturbation (either fluorine, hydrogen, or lithium).

	Fluorine (Ref. 22)	Hydrogen (Ref. 23)	Lithium (this work)
g_1	1.9746	1.9765	1.9688
g_2	1.9782	1.9732	1.9204
g_3	1.9430	1.9405	1.9323

the same pattern. For both fluorine and hydrogen, there are two larger values and one smaller value. The situation is reversed for the Ti^{3+}-Li^+ center where there is one larger value and two smaller values. This modest, but significant, difference is related to the relative energies of the d orbitals on the Ti^{3+} ions (see Fig. 8 in Ref. 22) and is a reflection of slight changes in the crystalline electric field at the Ti^{3+} ions. For all three defects, the $|x^2–y^2\rangle$ orbital is the ground state of the Ti^{3+} ion, and the $|z^2\rangle$ and $|xy\rangle$ orbitals have much higher energies. Here, we use an x, y, z coordinate system that has x along the $[\bar{1}10]$ direction, y along the [001] direction, and z along the [110] elongation direction of the TiO_6 octahedron in the rutile-structured crystal. Using the analysis in Ref. 22, we find that the $|xz\rangle$, $|yz\rangle$, and $|xy\rangle$ orbitals for the lithium center are approximately 2640, 2260, and 22100 cm^{-1}, respectively, above the $|x^2–y^2\rangle$ ground state. In the fluorine and hydrogen centers, a larger separation in energy between the $|xz\rangle$ and $|yz\rangle$ orbitals and the $|x^2–y^2\rangle$ ground state was observed.

V. SUMMARY

A neutral Ti^{3+}-Li^+ complex has been identified in single crystals of TiO_2 (rutile) using EPR and ENDOR. These defects are formed when Li^+ ions diffuse into the crystals during post-growth treatments. The Li^+ ions occupy an interstitial position and the charge-compensating electron is localized on an adjacent titanium ion at a regular site in the lattice. Principal values less than 2.0023 characterize the g matrix (as expected for a Ti^{3+} ion), while a classical point-dipole model describes the ^7Li hyperfine matrix. It is appropriate to view this Ti^{3+}-Li^+ complex as a donor-bound small polaron where the emphasis is placed on the Ti^{3+} ion.[24] With the inclusion of the present lithium-related defect, there is now a set of three similar, yet distinct, donor-bound small polaron centers (fluorine, hydrogen, and lithium) that have been reported in TiO_2 (rutile) crystals.[22,23] Another aspect of the present study relates to the mode by which Li^+ ions may diffuse along the c axis in this material, i.e., a "hopping" of the electron on the Ti sublattice correlated with the movement of the Li^+ ion from one interstitial site to the next. The accompanying extra charge-compensating electron may be important when describing or modeling the diffusion of Li^+ ions in TiO_2 crystals.

ACKNOWLEDGMENTS

The authors wish to acknowledge helpful discussions with Shan Yang during the initial phase of this project. One of the authors (A.T.B.) thanks the National Research Council for the award of a Postdoctoral Fellowship at the Air Force Institute of Technology. The research at West Virginia University was supported by Grant No. DMR-0804352 from the National Science Foundation.

[1]A. Fujishima, X. Zhang, and D. A. Tryk, Surf. Sci. Rep. **63**, 515 (2008).
[2]G. Liu, L. Wang, H. G. Yang, H.-M. Cheng, and G. Q. Lu, J. Mater. Chem. **20**, 831 (2010).
[3]M. K. Nowotny, L. R. Sheppard, T. Bak, and J. Nowotny, J. Phys. Chem. C **112**, 5275 (2008).
[4]M. Ni, M. K. H. Leung, D. Y. C. Leung, and K. Sumathy, Renewable Sustainable Energy Rev. **11**, 401 (2007).
[5]J. J. Yang, M. D. Pickett, X. Li, D. A. A. Ohlberg, D. R. Stewart, and R. S. Williams, Nat. Nanotechnol. **3**, 429 (2008).
[6]Z. Yang, D. Choi, S. Kerisit, K. M. Rosso, D. Wang, J. Zhang, G. Graff, and J. Liu, J. Power Sources **192**, 588 (2009).
[7]Y. Hu, L. Kienle, Y. Guo, and J. Maier, Adv. Mater. **18**, 1421 (2006).
[8]D. Wang, D. Choi, Z. Yang, V. V. Viswanathan, Z. Nie, C. Wang, Y. Song, J. Zhang, and J. Liu, Chem. Mater. **20**, 3435 (2008).
[9]P. Kubiak, M. Pfanzelt, J. Geserick, U. Hörmann, N. Hüsing, U. Kaiser, and M. Wohlfahrt-Mehrens, J. Power Sources **194**, 1099 (2009).
[10]A. Stashans, S. Lunell, R. Bergström, A. Hagfeldt, and S. Lindquist, Phys. Rev. B **53**, 159 (1996).
[11]M. V. Koudriachova, N. M. Harrison, and S. W. de Leeuw, Phys. Rev. B **65**, 235423 (2002).
[12]M. V. Koudriachova, S. W. de Leeuw, and N. M. Harrison, Phys. Rev. B **69**, 054106 (2004).
[13]J. H. Richter, A. Henningsson, P. G. Karlsson, M. P. Anderson, P. Uvdal, H. Siegbahn, and A. Sandell, Phys. Rev. B **71**, 235418 (2005).
[14]W. J. H. Borghols, D. Lützenkirchen-Hecht, U. Haake, E. R. H. van Eck, F. M. Mulder, and M. Wagemaker, Phys. Chem. Chem. Phys. **11**, 5742 (2009).
[15]B. J. Morgan and G. W. Watson, Phys. Rev. B **82**, 144119 (2010).
[16]B. J. Morgan and P. A. Madden, Phys. Rev. B **86**, 035147 (2012).
[17]H. Yildirim, J. P. Greeley, and S. K. R. S. Sankaranarayanan, Phys. Chem. Chem. Phys. **14**, 4565 (2012).
[18]J. Yu, M. L. Sushko, S. Kerisit, K. M. Rosso, and J. Liu, J. Phys. Chem. Lett. **3**, 2076 (2012).
[19]C. Di Valentin, G. Pacchioni, and A. Selloni, J. Phys. Chem. C **113**, 20543 (2009).
[20]S. Yang, L. E. Halliburton, A. Manivannan, P. H. Bunton, D. B. Baker, M. Klemm, S. Horn, and A Fujishima, Appl. Phys. Lett. **94**, 162114 (2009).
[21]F. D. Brandao, M. V. B. Pinheiro, G. M. Ribeiro, G. Medeiros-Rebeiro, and K. Krambrock, Phys. Rev. B **80**, 235204 (2009).
[22]S. Yang and L. E. Halliburton, Phys. Rev. B **81**, 035204 (2010).
[23]A. T. Brant, Shan Yang, N. C. Giles, and L. E. Halliburton, J. Appl. Phys. **110**, 053714 (2011).
[24]F. Bekisli, W. B. Fowler, and M. Stavola, Phys. Rev. B **86**, 155208 (2012).
[25]S. Yang, "Paramagnetic resonance studies of defects in titanium dioxide crystals," Ph.D. Dissertation (West Virginia University, Morgantown, WV, 2009).
[26]J. A. Weil and J. R. Bolton, *Electron Paramagnetic Resonance: Elementary Theory and Practical Applications*, 2nd ed. (Wiley-Interscience, John Wiley and Sons, New York, 2007), Chap. 12.
[27]M. G. Jani, L. E. Halliburton, and A. Halperin, Phys. Rev. Lett. **56**, 1392 (1986).
[28]J. R. Morton and K. F. Preston, J. Magn. Reson. (1969-1992) **30**, 577 (1978).
[29]J. A. J. Fitzpatrick, F. R. Manby, and C. M. Western, J. Chem. Phys. **122**, 084312 (2005).
[30]F. J. Adrian, A. N. Jette, and J. M. Spaeth, Phys. Rev. B **31**, 3923 (1985).